

Carbon corrosion characteristics of CN_x nanostructures in acidic media and implications for ORR performance

Dieter von Deak · Elizabeth J. Biddinger · Umit S. Ozkan

Received: 22 May 2010/Accepted: 17 March 2011/Published online: 6 April 2011
© Springer Science+Business Media B.V. 2011

Abstract Accelerated electrochemical corrosion of nitrogen-containing carbon (CN_x) oxygen reduction catalysts was performed by a chronoamperometric hold at 1.2 V versus NHE in acidic electrolyte using a rotating disk electrode system. Cyclic voltammograms were used to measure the electrochemically active quinone/hydroquinone redox reaction couple indicating the degree of carbon corrosion. Half-cell testing of CN_x oxygen reduction catalyst materials showed superior carbon corrosion resistance compared to Vulcan carbon, the most ubiquitous cathode catalyst support. When oxygen reduction activity was measured before and after carbon corrosion, carbon corrosion resilience trended with the oxygen reduction activity. CN_x catalysts subjected to carbon corrosion testing did not show a change in the onset of oxygen reduction reaction (ORR) activity potentials with only a slight reduction in current density, but showed improved ORR selectivity to the complete reduction of dioxygen to water.

Keywords Carbon corrosion · Fuel cell · Oxygen reduction reaction · Cathode catalyst · Quinone/hydroquinone

1 Introduction

Proton exchange membrane (PEM) fuel cells have the potential to greatly impact the portable energy utilization sector, but there are technological hurdles that must be

addressed before PEM fuel cells become market-ready. Currently, costly platinum and platinum alloy catalysts with high loadings are utilized to accelerate the slow kinetics of the oxygen reduction reaction (ORR) on the cathode side of the fuel cell. Inexpensive nitrogen-doped carbon catalysts have been shown to have significant ORR activity (which is less than expensive platinum-based catalysts) [1–18], but understanding the process by which these catalyst materials deactivate is necessary for further development [14, 19].

Carbon materials are commonly used as a support for platinum and platinum-alloyed cathode catalysts in PEM fuel cells. Carbon support materials are chosen due to their economics, high surface area, thermal and electrical conductivity, and high stability under normal PEM fuel cell operating conditions [20, 21]. Corrosive conditions in PEM fuel cells occur at low pH (<1) [22], high temperatures (50–90 °C) [22], high operating potential (0.6–1.2 V) [22] and low hydrogen feed concentrations [21]. These conditions prevail especially when the fuel cell is at open circuit voltage (OCV), where exchange currents are high and the cathode is subjected to potentials in excess of 1.2 V versus NHE [20, 21]. Although, fuel cell operating conditions appear to make the carbon support prone to carbon corrosion, in practice, the actual carbon corrosion is slow [20, 23]. During normal fuel cell operation an excess of protons are available in the cathode making oxygen reduction the preferred reaction compared to carbon oxidation, due to Le Chatelier's principle. The oxygen reduction and carbon corrosion reactions involved are shown in Scheme 1.

There are two main electrochemical methods employed to accelerate carbon corrosion for ORR catalysts in half-cell and fuel cell experiments. One method employs cyclic voltammograms (CVs) that cycle from 1.2–1.4 V versus NHE to approximately 0 V versus NHE at fixed rate with

D. von Deak · E. J. Biddinger · U. S. Ozkan (✉)
Department of Chemical and Biomolecular Engineering,
The Ohio State University, Columbus, OH 43210, USA
e-mail: ozkan.1@osu.edu

| | | |
|------------------|---|----------------|
| Carbon Corrosion | $C + 2H_2O \rightarrow CO_2 + 4H^+ + 4e^-$ | 0.207V vs. NHE |
| | $C + H_2O \rightarrow CO + 2H^+ + 2e^-$ | 0.518V vs. NHE |
| | $C + 2H_2O \rightarrow HCOOH + 2H^+ + 2e^-$ | 0.523V vs. NHE |
| Oxygen Reduction | $O_2 + 2H^+ + 2e^- \rightarrow H_2O_2$ | 0.695V vs. NHE |
| | $O_2 + 4H^+ + 4e^- \rightarrow 2H_2O$ | 1.229V vs. NHE |

Scheme 1 Carbon corrosion and oxygen reduction reactions and their standard potentials

or without rest periods between cycles for the duration of the test [20, 22–27]. Cycling voltage has shown a reduction in fuel cell performance for noble metal ORR catalysts and was used to demonstrate the carbon corrosion resistance of support media for the noble metal [28]. However, it has been shown that voltage cycling can lead to detachment of Pt nanoparticles without corroding the carbon support perceptibly [24]. Furthermore, repeated CV techniques were shown to preferentially corrode the carbon sublayer that is between the active catalyst layer and the gas diffusion layer due to high potential and low hydrogen concentration, instead of the cathode catalyst layer [20]. The other electrochemical technique used to measure carbon corrosion is a chronoamperometric hold at high potential (1.2–1.4 V vs. NHE) with intermediate activity or CV testing to monitor the progress of the carbon corrosion [21, 29–33]. The chronoamperometric technique has been shown to increase the surface oxide concentration [33], which is an intermediate step in the corrosion of carbon materials before the formation of carbon dioxide gas [34]. Chronoamperometric techniques have also shown a decrease in activity of Pt/C ORR cathode catalyst with duration of potential hold [29, 32, 33].

Carbon corrosion has been studied for various carbon support materials with [31, 34] and without Pt catalysts [29, 32], but the corrosion of nitrogen-doped carbon ORR catalysts in acidic medium simulating the PEM fuel cell environment, to our knowledge, has not been studied directly. Unfortunately the deactivation of Pt/C catalysts are due to multiple effects; Pt agglomeration, Pt nanoparticle detachment, and carbon corrosion. Furthermore, the capacitance current of platinum oxide groups obscures the location of the hydroquinone/quinone at 0.6 V versus NHE in the cathodic scan of a cyclic voltammogram. In this study, we have chosen to examine the corrosion behavior of Vulcan carbon as well as CN_x catalysts. Furthermore, since fuel cell operation will experience high cathode potentials during OCV and lean fuel operation during startup, chronoamperometry was chosen to examine the carbon corrosion of CN_x catalyst materials. Due to the compounding complications in platinum catalyst the focus of this publication is to elucidate the corrosion resistance of Pt-free, nitrogen-doped graphite ORR catalysts as they compare to Vulcan carbon, the most prevalent type of carbon support used in fuel cells.

2 Experimental

2.1 Catalyst synthesis

The CN_x catalysts were synthesized by pyrolyzing acetonitrile over a metal oxide or carbon support material. The oxide support used was a MgO nanopowder (Aldrich), either doped with 2 wt% Fe using DI water and iron acetate (Aldrich) solution through incipient wetness impregnation technique, or used as received. Fe-doped (2 wt%) Vulcan carbon was prepared using a similar wet impregnation procedure. The resulting material was purged with nitrogen gas at 150 ccm for 30 min at room temperature and then heated to 900 °C at 10 °C min⁻¹. Once the furnace temperature reached 900 °C, the nitrogen gas was saturated with acetonitrile and subjected to a 2-h catalyst growth period in which CN_x nano-structures were grown. Upon completion of the growth period, the material was allowed to rapidly cool to 23 °C with N₂ flowing. Catalysts containing a magnesia support were washed in 1 M HCl for 1 h at 60 °C with agitation to remove any exposed support and metals. The washed catalyst was then rinsed with a ~1000 mL of DI H₂O and allowed to dry in air at 110 °C. Upon drying, the resulting nitrogen-containing graphitic carbon ORR catalyst is denoted as CN_x. Additional details on CN_x catalyst synthesis have been reported previously [1, 5]. The relative surface composition of CN_x grown on Fe/MgO determined through X-ray photoelectron spectroscopy was 86.1% carbon, 9.0% nitrogen, 3.4% oxygen, and 0.1% magnesium [3]. The resulting materials produced were mainly stacked cup nanostructures for CN_x grown on Fe/MgO, herringbone nanostructures for CN_x grown on Fe/VC and nanocubes for CN_x grown on MgO [1, 5]. The nanostructure of Vulcan carbon tends to be a nano onion-type geometry. The nanostructure of catalysts and support materials likely affects the ORR on the surface [1].

2.2 Carbon corrosion measurement

Cyclic voltammograms were used to measure the current of the electrochemically active quinone/hydroquinone redox reaction indicating the degree of carbon corrosion using a PAR bipotentiostat. To simulate the fuel cell environment, half-cell corrosion tests were performed in fresh 0.5 M H₂SO₄ with a rotating ring disk electrode (RRDE) (PAR Model 636 Electrode Rotator). An Ag/AgCl (Sat. KCl) (Gamry Instruments) reference electrode was used to measure potential. A platinum wire counter electrode was also used in the half-cell setup. Argon was continuously sparged through the 0.5 M H₂SO₄ electrolyte during testing and at least 30 min before testing so that changes in the oxygen reduction activity would not mask the detection of the quinone/hydroquinone species. A catalyst ink was

prepared by mixing 1:10:160 catalyst: 5% Nafion in aliphatic alcohols (Electrochem): 100% ethanol (Decon) by weight and was immediately sonicated for 30 min. After sonication, three 5 μL aliquots of catalyst ink were applied to the glassy carbon (GC) disk electrode of the RRDE (MT28 Series ThinGap RRDE Pine Research), allowing the ink to dry between applications. Assuming uniform dilution of the ink, this catalyst loading was 426 $\mu\text{g cm}^{-2}$. Once the catalyst-coated electrode had dried, it was wetted with DI H_2O before being submerged in the 0.5 M H_2SO_4 electrolyte. Carbon corrosion was accelerated by holding the catalyst-coated electrode at 1.2 V versus NHE for 48 h. The progress of carbon corrosion was monitored by intermittent CVs from 1.2 V to 0.2 V to 1.2 V versus NHE at 10 mV sec^{-1} after 0, 2, 4, 8, 16, 24, and 48 h of accelerated carbon corrosion. A series of five CVs was used at each carbon corrosion interval to ensure that the recorded signal had reached steady state. All corrosion comparisons were done using steady state CVs. The intermittent CVs were used to measure the evolution of the hydroquinone/quinone with time of potential hold. All corrosion tests were performed at 1000 rpm and at room temperature, $23 \pm 1^\circ\text{C}$. Similar investigations have been performed that demonstrate carbon corrosion on Pt on carbon [29, 33] and carbon nanotubes [31]. It should be pointed out that in a membrane electrode assembly the carbon gas diffusion layer is especially susceptible to carbon corrosion [20], so the following study has focused solely on cathode catalyst materials.

2.3 Activity-selectivity measurements (ORR)

The ORR activity and selectivity data were collected using the rotating ring disk (RRDE) technique in an O_2 -saturated half-cell of 0.5 M H_2SO_4 . Catalyst ink was applied to the GC disk of the RRDE in the same manner as described in the Sect. 2.2. The thin hydrophobic Teflon ring in the MT28 Series ThinGap RRDE electrode tip (Pine Research) separated the GC disk from the platinum ring which allowed the hydrophilic catalyst ink to only be deposited GC disk and not on platinum ring. Oxygen was bubbled through the half-cell electrolyte for more than 30 min to reach saturation. Once the electrode was submerged into the O_2 -saturated 0.5 M H_2SO_4 electrolyte, two cyclic voltammograms from 1.2 V to 0.0 V to 1.2 V versus NHE at 10 mV s^{-1} were performed to wet the electrode surface. The electrolyte was

then saturated with argon gas by sparging for a minimum of 30 min. A series of CVs were performed on the catalyst-coated disk electrode from 1.2 V to 0 V to 1.2 V versus NHE at 50 mV s^{-1} while holding the Pt ring at 1.2 V versus NHE to remove surface impurities from both the disk and ring until reproducible scans were reached. Next, an ORR activity background was collected in argon-saturated electrolyte by scanning at 10 mV s^{-1} from 1.2 V to 0.0 V to 1.2 V versus NHE at 100 rpm while holding the ring at 1.2 V versus NHE. The electrolyte was then bubbled with pure oxygen for more than 30 min. Once again, a series of CVs was done on the catalyst-coated disk electrode from 1.2 V to 0.0 V to 1.2 V versus NHE at 50 mV s^{-1} while holding the Pt ring at 1.2 V versus NHE to remove surface impurities from both the disk and ring until reproducible scans were acquired. Next, ORR activity-selectivity data were collected by scanning at 10 mV s^{-1} from 1.2 V to 0 V to 1.2 V versus NHE while holding the ring at 1.2 V versus NHE at 100, 0, and 1000 rotations per minute.

Selectivity is determined as the number of electrons transferred per oxygen molecule reduced at the disk (n) by evaluating the difference in the disk and ring currents during ORR testing. An n value of 4 corresponds to a complete reduction of dioxygen to water with a four-electron transfer, while an n value of 2 is equivalent 100% selectivity to hydrogen peroxide formation.

The reactions measured through the disk current are the desired full reduction of dioxygen and the partial reduction of dioxygen to form H_2O_2 , respectively [35].



The ring was held at 1.2 V versus NHE, where ORR current is negligible and the oxidation of H_2O_2 to oxygen is mass transfer limited.

Selectivity, n , is calculated using the following equation:

$$n = \frac{4I_D}{I_D + \left(\frac{I_R}{N}\right)},$$

where n = number of electrons transferred per oxygen molecule, I_D = disk current of the ORR reaction, I_R = ring current, and N = collection efficiency of the ring (0.22 for RRDE tip used).

Table 1 shows the three types of electrochemical experiments performed. An ORR test is an activity-

Table 1 The types of electrochemical experiments performed

| Test type | Consecutive experimental procedures | | |
|-------------------|-------------------------------------|--------------------------|--------------------------|
| ORR | Ink application | Oxygen reduction testing | |
| Corrosion | Ink application | Corrosion testing | |
| ORR-corrosion-ORR | Ink application | Oxygen reduction testing | Corrosion testing |
| | | | Oxygen reduction testing |

selectivity measurement on freshly applied catalyst. A corrosion test is a carbon corrosion measurement on a freshly applied catalyst. An ORR-corrosion-ORR test is an ORR activity-selectivity measurement on freshly applied catalyst followed by a carbon corrosion measurement and another activity-selectivity measurement on the same catalyst-coated electrode.

3 Results and discussion

3.1 Carbon corrosion on CN_x materials and Vulcan carbon (corrosion tests)

The degree of carbon corrosion was determined by observing the evolution of the quinone to hydroquinone peak in the anodic scan of intermittent CVs while performing chronoamperometric potential holds at 1.2 V versus NHE over 48 h in a RDE experimental setup in 0.5 M H_2SO_4 electrolyte. Vulcan carbon has been shown to oxidize in sulfuric acid with high potential holds and undergo the intermediate hydroquinone/quinone species during carbon corrosion [29–31]. Graphitic carbon materials all have some degree of oxygen functionalization at ambient conditions [36]. As carbon is corroded, formation of additional oxygen functional groups can indicate carbon corrosion. Since Vulcan carbon and CN_x ORR catalysts are both primarily graphitic carbon, it is reasonable that CN_x would corrode through a similar mechanism and therefore corrosion resistance could be gauged by high potential holds in sulfuric acid.

The quinone/hydroquinone oxidation reduction reaction can be seen in Fig. 1a. Figure 1b shows the intermittent CVs taken over Vulcan carbon while performing chronoamperometric potential holds. The quinone/hydroquinone peaks are evident by the increase in current at ~ 0.6 V versus NHE [29, 30] with time in the anodic (upper) set of linear scans. The intensity of the peaks increases significantly as the duration of high-voltage hold increases. Figure 1c shows similar CVs taken over CN_x grown on Fe-doped Vulcan carbon. The intensity increase of quinone/hydroquinone peaks in CN_x materials is smaller than Vulcan carbon, suggesting that these materials are more corrosion resistant.

Figure 2a shows a comparison of the corrosion behaviors of three different CN_x catalysts grown on different supports and untreated Vulcan carbon. The extent of corrosion is expressed as percent change in the intensity of the quinone/hydroquinone electrochemically active couple (at 0.627 V vs. NHE) in the anodic current of intermittent CVs with increasing duration of the potential hold of 1.2 V versus NHE. The high increase in the quinone/hydroquinone peak over Vulcan carbon indicates that Vulcan carbon

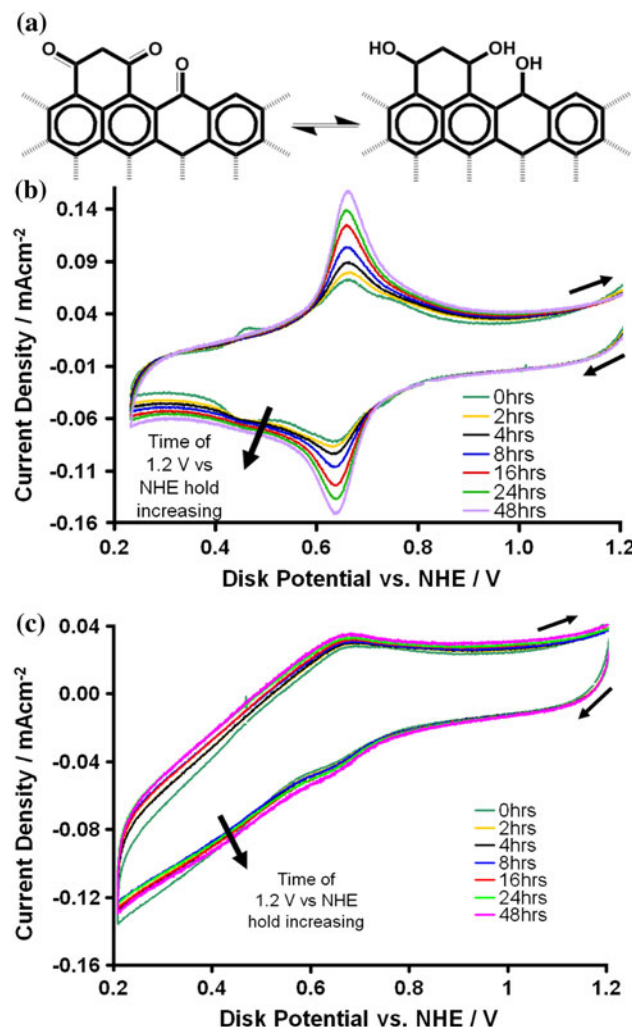


Fig. 1 (a) Electrochemically active quinone (left)-hydroquinone (right) reduction-oxidation couple on graphite edge, (b) Evolution of the quinone/hydroquinone species on Vulcan Carbon-XC72, (c) evolution of the hydroquinone/quinone species on CN_x grown on Fe/Vulcan carbon. CVs are taken after 0, 2, 4, 8, 16, 24, 48 hrs with 1.2 V vs. NHE potential hold in 0.5 M H_2SO_4 (1000 rpm, 10 mV/sec, 426 $\mu\text{g}/\text{cm}^2$ catalyst loading)

is much less corrosion resistant than CN_x ORR catalyst materials. The small growth of the quinone/hydroquinone peak for “ CN_x grown on Fe/MgO” and “ CN_x grown on Fe/Vulcan Carbon” indicates that iron-catalyzed growth of CN_x leads to an increase in carbon corrosion resistance of the ORR catalysts. The increased corrosion resistance may be due to an increase in graphitic character of these materials as well as the increased nitrogen functionalities on the edges. Previous studies have shown that CN_x nanostructures formed during pyrolysis have a higher degree of edge plane exposure and a higher degree of pyridinic nitrogen when transition metals (Fe, Co) are used to catalyze the growth CN_x catalyst [3]. Although carbon corrosion is thought to attack the chemically active edges

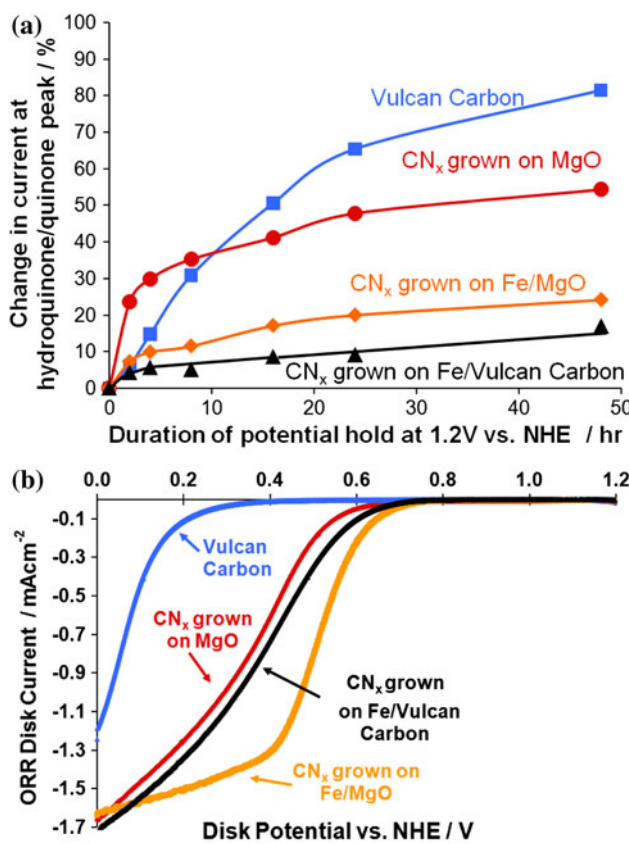


Fig. 2 (a) Carbon corrosion of CN_x catalysts and Vulcan carbon support reported as change in the intensity of the quinone/hydroquinone electrochemically active couple (at 0.627 V vs. NHE) in the anodic current of intermittent CVs with potential hold of 1.2 V vs. NHE in a rotating disk electrode experimental setup, (b) ORR activity of the same four catalysts, (1000 rpm, 10 mV/sec, 426 $\mu\text{g}/\text{cm}^2$ catalyst loading)

of graphite [29, 37], the observation that CN_x catalysts with high edge plane exposure have a higher resistance to carbon corrosion would suggest that the inclusion of nitrogen into graphite could potentially reduce the oxidation of the exposed edge planes and retard carbon corrosion.

Figure 2b shows a comparison of the ORR activity of the same four materials used for corrosion testing. As expected, CN_x catalysts were found to have much greater oxygen reduction activity than Vulcan carbon. Nitrogen functionalities imparted to these CN_x materials through pyrolysis in nitrogen and carbon containing atmospheres is known to increase their oxygen reduction activity [15, 38]. CN_x ORR catalysts grown over Fe-doped supports were found to have a higher ORR activity than CN_x formed without iron-catalyzed growth. This increase in activity may be due to the formation of carbon–nitrogen nanostructures that have more edge plane exposure per mass [3], which is where oxygen reduction likely takes place [1, 6, 10, 39]. Another correlation that has been reported

previously is between the ORR activity and the pyridinic nitrogen content of the CN_x materials [2, 7, 40].

The two comparisons shown in Fig. 2a and b reveal that catalysts with higher ORR activity exhibit the increased resistance to carbon corrosion. In other words, the catalysts with the highest oxygen reduction activity are the most resistant to carbon corrosion. This trend was persistent in all catalysts studied. This could be due to the catalyst's ability to preferentially facilitate the reduction of oxygen over the surface instead of carbon oxidation reactions that would lead to carbon corrosion.

3.2 Effect of corrosion on the ORR (ORR-corrosion-ORR tests)

In an effort to observe the effect of carbon corrosion on ORR performance of these materials, the RRDE oxygen reduction activity and selectivity tests were performed before and after electrochemical corrosion testing. The same electrocatalyst electrode was submitted to all three electrochemical tests in succession, so currents could be compared directly and unambiguously. A comparison of the disk and ring currents obtained before and after corrosion tests is presented in Fig. 3a for the most active (CN_x grown on Fe/MgO) and the least active (Vulcan carbon support) ORR catalysts. The selectivities calculated using disk and ring currents are expressed as number of electrons transferred per O₂ molecule (*n*), and shown in Fig. 3b for these two catalysts before and after corrosion testing. For the CN_x grown on Fe/MgO, the ORR activity current density was slightly lower following corrosion testing although the onset of activity did not change. Vulcan carbon did not show much ORR activity loss, however, the activity was extremely low to start with. Another observation is that the selectivity of the most active catalyst improved following corrosion testing (*n* increasing from ~3.7 to 3.9) while that of Vulcan carbon somewhat decreased. This could be due in part to an increase in oxygen function groups [17, 41], which were observed electrochemically. Because the current density for Vulcan carbon was very low at voltages above 0.3 V versus NHE, the selectivity values were not reported in this range (Fig. 3b).

The effect of ORR activity testing on the corrosion behavior of the catalysts was examined by performing corrosion tests on fresh catalyst-coated electrodes and electrodes after ORR tests. Corrosion CVs taken on freshly applied catalysts and catalysts post-ORR testing after 0 or 48 h of hold time at high voltage are shown for CN_x grown on Fe/Vulcan carbon and untreated Vulcan carbon in Fig. 4a and b, respectively. Vulcan carbon and CN_x grown on Fe/Vulcan carbon catalyst both show a substantial decrease of the hydroquinone/quinone peak after ORR

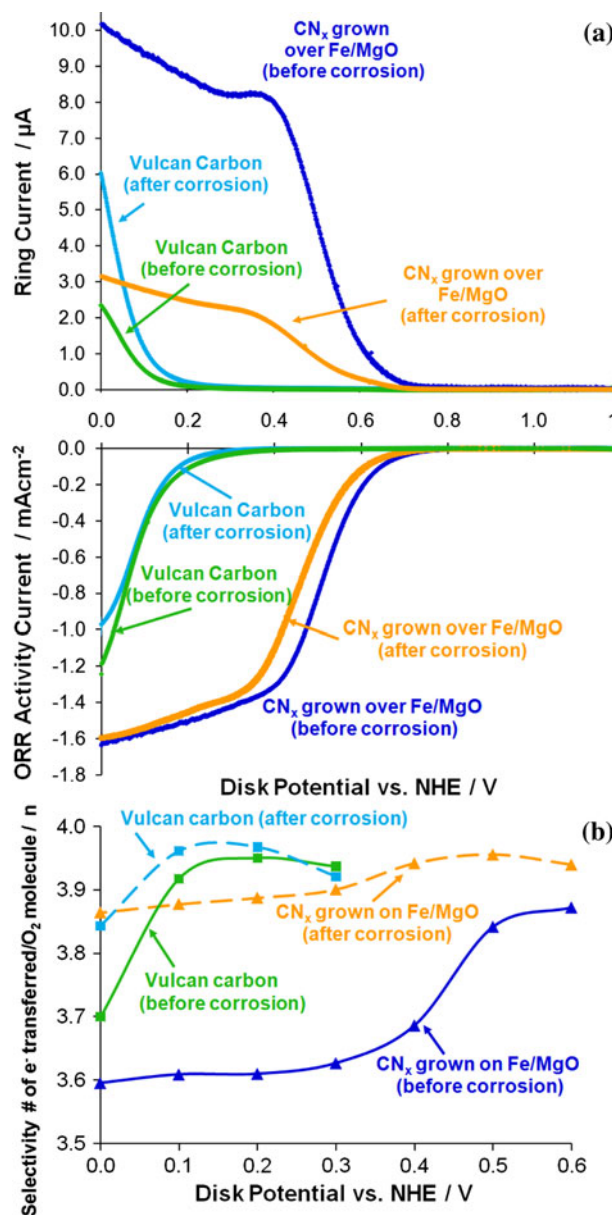


Fig. 3 RRDE activity and selectivity comparison before and after corrosion testing (a) (above) the ring current (a) (below) disk current density, (b) number of electrons transferred per O_2 molecule calculated from the ring and disk currents. Data collected in oxygen-saturated 0.5 M H_2SO_4 (1000 rpm with a catalyst loading 426 $\mu g/cm^2$, 10 mV/s) and the ring current at the Pt ring held at 1.2 V vs. NHE in oxygen saturated 0.5 M H_2SO_4 . Data are presented after Ar background is subtracted

testing. The relative intensity increase of the quinone/hydroquinone current during corrosion testing (from 0 to 48 h of hold time) did not change much for Vulcan carbon following ORR testing. CN_x grown on Fe/Vulcan carbon showed significantly less growth in the quinone/hydroquinone peak post ORR compared to fresh catalyst, but had a substantial decrease in the cathodic current at low potentials (Fig. 4a). The decrease in cathodic current at low

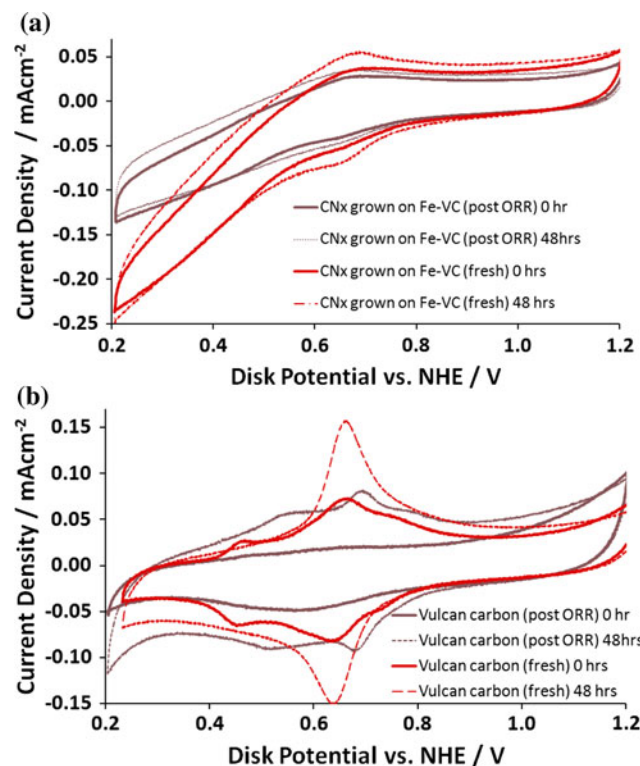


Fig. 4 Quinone/hydroquinone detection CVs after 0 and 48 hr 1.2 V vs. NHE potential holds for; (a) fresh and ORR tested CN_x grown on Fe/Vulcan carbon, (b) fresh and ORR tested Vulcan carbon-XC72. Tested in 0.5 M H_2SO_4 , at 1000 rpm, 10 mV/sec, 426 $\mu g/cm^2$ catalyst loading

potentials (0.5–0.2 V vs. NHE) during corrosion testing for materials subjected to ORR testing was unique to CN_x catalyst materials. This decrease in cathodic current at low potentials for CN_x grown on Fe/Vulcan carbon post-ORR testing can be attributed to a removal of surface oxides apart from the electrochemically active quinone/hydroquinone species [34, 42]. ORR testing appears to have consumed much of electrochemically active quinone/hydroquinone and low cathodic potential oxygen species present on the catalyst surface (Fig. 4), suggesting a surface stabilization during ORR testing, which makes it less prone to carbon corrosion.

4 Conclusions

The CN_x ORR catalyst materials showed superior carbon corrosion resistance compared to Vulcan carbon, which is the most commonly used carbon material in fuel cells. CN_x materials grown on an iron-doped support had higher ORR activity than materials subjected to an acetonitrile atmosphere at high temperature without an iron growth catalyst. CN_x catalysts subjected to carbon corrosion testing did not show a change in the potentials of activity onset only a

slight reduction in current density, but exhibited improved ORR selectivity to the complete reduction of dioxygen to water. Carbon corrosion resistance trended with increasing oxygen reduction activity with the most active CN_x catalysts showing the most resistance to corrosion. These CN_x catalysts also became more resistant to carbon corrosion following ORR activity measurements, possibly due to surface stabilization during the ORR.

Acknowledgments The authors gratefully acknowledge the support for this study from the US Department of Energy—Basic Energy Sciences through the grant # DE-FG02-07ER15896.

References

1. Matter PH, Zhang L, Ozkan US (2006) J Catal 239:83
2. Lefevre M, Proietti E, Jaouen F, Dodelet J-P (2009) Science 324:71
3. Matter PH, Wang E, Arias M, Biddinger EJ, Ozkan US (2007) J Mol Catal 264:73
4. Matter PH, Biddinger EJ, Ozkan US (2007) Non-precious metal oxygen reduction catalysts for PEM fuel cells. The Royal Society of Chemistry, Cambridge
5. Matter PH, Wang E, Ozkan US (2006) J Catal 243:395
6. Matter PH, Wang E, Arias M, Biddinger EJ, Ozkan US (2006) J Phys Chem B 110:18374
7. Matter PH, Ozkan US (2006) Catal Lett 109:115
8. Bezerra CWB, Zhang L, Lee K, Liu H, Marques ALB, Marques EP, Wang H, Zhang J (2008) Electrochim Acta 53:4937
9. Nallathambi V, Lee J-W, Kumaraguru SP, Wu G, Popov BN (2008) J Power Sources 183:34
10. Subramanian NP, Li X, Nallathambi V, Kumaraguru SP, Colon-Mercado H, Wu G, Lee J-W, Popov BN (2009) J Power Sources 188:38
11. Wu G, Chen Z, Artyushkova K, Garzon FH, Zelenay P (2008) ECS Trans 16:159
12. Schilling T, Bron M (2008) Electrochim Acta 53:5379
13. Chung HT, Johnston CM, Garzon FH, Zelenay P (2008) ECS Trans 16:385
14. Gasteiger HA, Markovic NM (2009) Science 324:48
15. Shao Y, Sui J, Yin G, Gao Y (2008) Appl Catal B Environ 79:89
16. Bashyam R, Zelenay P (2006) Nature 443:63
17. Biddinger EJ, von Deak D, Ozkan US (2009) Top Catal 52:1566
18. Maldonado S, Stevenson KJ (2005) J Phys Chem B 109:4707
19. Jaouen F, Herranz J, Lefevre M, Dodelet J-P, Kramm UI, Herrmann I, Bogdanoff P, Maruyama J, Nagaoka T, Garsuch A, Dahn JR, Olson TS, Pylypenko S, Atanassov P, Ustinov EA (2009) ACS Appl Mat Interfaces 1:1623
20. Young AP, Stumper J, Gyenge E (2009) J Electrochem Soc 156:B913
21. Kim J, Lee J, Tak Y (2009) J Power Sources 192:674
22. Roen LM, Paik CH, Jarvi TD (2004) Electrochim Solid State Lett 7:A19
23. Chaparro AM, Mueller N, Atienza C, Daza L (2006) J Electroanal Chem 591:67
24. Mayrhofer KJJ, Meier JC, Ashton SJ, Wiberg GKH, Kraus F, Hanzlik M, Arenz M (2008) Electrochim Commun 10:1144
25. Weng F-B, Hsu C-Y, Li C-W (2010) Int J Hydrogen Energy 35:3664
26. Oh H-S, Kim K, Ko Y-J, Kim H (2010) Int J Hydrogen Energy 35:701
27. Liu ZY, Zhang JL, Yu PT, Zhang JX, Makharia R, More KL, Stach EA (2010) J Electrochim Soc 157:B906
28. Li X, Park S, Popov BN (2010) J Power Sources 195:445
29. Li L, Xing Y (2006) J Electrochim Soc 153:A1823
30. Kangasniemi KH, Condit DA, Jarvi TD (2004) J Electrochim Soc 151:E125
31. Shao Y, Yin G, Zhang J, Gao Y (2006) Electrochim Acta 51:5853
32. Wang X, Li W, Chen Z, Waje M, Yan Y (2006) J Power Sources 158:154
33. Wang J, Yin G, Shao Y, Zhang S, Wang Z, Gao Y (2007) J Power Sources 171:331
34. Li L, Xing Y (2008) J Power Sources 178:75
35. Bard AJ, Faulkner LR (2001) Electrochemical methods: fundamentals and applications. Wiley, New York
36. Boehm HP (1994) Carbon 32:759
37. Toebees ML, van Heeswijk JMP, Bitter JH, van Dillen AJ, de Jong KP (2004) Carbon 42:307
38. Cote R, Lalonde G, Guay D, Dodelet JP, Denes G (1998) J Electrochim Soc 145:2411
39. Jaouen F, Marcotte S, Dodelet J-P, Lindbergh G (2003) J Phys Chem B 107:1376
40. Wang P, Ma Z, Zhao Z, Jia L (2007) J Electroanal Chem 611:87
41. Biddinger EJ, Knapke DS, von Deak D, Ozkan US (2010) Appl Catal B Environ 96:72
42. Kinoshita K, Bett JAS (1974) Carbon 12:525